Sustainable Cities and Society 113 (2024) 105710

Contents lists available at ScienceDirect

Sustainable Cities and Society

journal homepage: www.elsevier.com/locate/scs

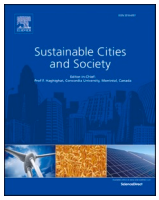

Resilience assessment of subway system to waterlogging disaster

Fei Xu [a,b], Delin Fang [a,b,*], Bin Chen [c], Hao Wang [d]

[a] State Key Laboratory of Earth Surface Processes and Resource Ecology, Beijing Normal University, Beijing 100875, China
[b] Faculty of Geographical Science, Beijing Normal University, Beijing 100875, China
[c] School of Environment, Beijing Normal University, Beijing 100875, China
[d] Faculty of Architecture, Civil and Transportation Engineering, Beijing University of Technology, Beijing 100124, China

ARTICLE INFO

Keywords:
Resilience assessment
Subway system waterlogging
Stability-Resistance-Recovery
EWM-TOPSIS

ABSTRACT

The subway system is experiencing significant waterlogging challenges due to climate change and urbanization, and the enclosed underground structure makes this issue worsen. Identification of subway system waterlogging resilience (SSWR) and the development of improvement measures are critical. We proposed a "Stability-Resistance-Recovery" assessment framework of the SSWR based on the system performance curve. An integrated index system was established, which defined and quantified several indexes to capture unique characteristics of subway systems. The system used inundation results simulated by InfoWorks ICM model as trigger for waterlogging, providing accurate reflection of inundation situations around subway stations. A case study in Beijing identified the stability and resistance as the leading factors affecting the SSWR, with water bodies surface percentage, evening peak departure time interval, and population density having the strongest impacts. Subway system exhibited a relatively low level of waterlogging resilience, with 51.9% of stations indicating very low or low levels. Stations at medium SSWR were dispersed throughout the areas neighboring stations at very low or low SSWR. Stations at very high or high SSWR were minimal and scattered in peripheral areas. This study provides a widely applicable index system for the SSWR and helps decision-makers devise the improvement measures.

1. Introduction

As a result of global climate change and rapid urban development, waterlogging has emerged as one of the most frequent natural disasters worldwide (D'Ambrosio and Longobardi, 2023; Lu et al., 2022; Ziari et al., 2023), causing enormous casualties and property loss (Qi and Zhang, 2022; Zhang et al., 2021). To mitigate urban waterlogging, various strategies such as rain gardens, green roofs (as green infrastructure), open detention basins (as blue infrastructure), and pipelines (as gray infrastructure) are all considered effective in reducing runoff and mitigating waterlogging losses (Damodaram and Zechman, 2013; Alves et al., 2019). For instance, Zhao et al. demonstrated the effectiveness of urban waterlogging control through the updating and optimization the spatial layout of impervious surface (Zhao et al., 2024).

To alleviate the transportation pressure caused by urban expansion, the extensive construction and utilization of underground spaces and infrastructure have become an inevitable trend (Lin et al., 2023; Qiao et al., 2024). As a vital component of the underground infrastructure, the extensive construction of subway system has significantly improved the quality of life for residents and ensure the smooth operation of cities. There is no denying the fact that the increasing waterlogging disaster greatly poses a significant threat to the safety of the subway system (Lyu et al., 2019b; Lyu et al., 2018). For example, on 30 July of 2023, affected by the residual circulation of Super Typhoon Duksuri, a rainstorm led to the closure of Tiananmen East Station, Tiananmen West Station, and Qianmen Station in Beijing, which seriously disrupted the normal operation of subway traffic. Moreover, compared to surface and elevated road traffic, the subway system is more susceptible to waterlogging due to its enclosed structure and high passenger density. Additionally, the system takes much longer to recover from waterlogging (Zhao et al., 2022) and even lead to a series of cascading failures (Yang et al., 2023). Therefore, it is imperative to place ample emphasis on the safe operation of subway systems during episodes of waterlogging, as this is essential for protecting people's lives and property.

The United Nations Office for Disaster Risk Reduction (UNDRR) pointed out in the Global Assessment Report (GAR) Special Report 2023 that, in an increasingly complex and hazardous world, resilience is the key to sustainable development today and in the future. The report

* Corresponding author: Delin Fang, No. 19, Xinjiekouwai St., Beijing, 100875, P R China Tel/Fax. : +86 10 58807368
E-mail address: fangd@bnu.edu.cn (D. Fang).

https://doi.org/10.1016/j.scs.2024.105710
Received 19 April 2024; Received in revised form 25 July 2024; Accepted 25 July 2024
Available online 26 July 2024

emphasizes the importance of enhancing resilience to cope with and withstand impacts. The "Beijing Resilient City Spatial Plan (2022-2035)" highlights the use of disaster simulation and forecasting to anticipate various "resilient planning" measures that can be implemented within the city. The goal is to actively mobilize resources and ensure the basic operation of essential urban functions, thereby strengthening the city's capacity to maintain operations during disasters and to recover afterward. Therefore, in order to strengthen the emergency maintenance and post-disaster recovery capabilities of subway system in the face of waterlogging and advance the sustainable development of the subway system, how to assess and improve the subway system waterlogging resilience (SSWR) has become an urgent issue that needs to be addressed (Jiao et al., 2023).

The rest parts of the study are organized as follows: the second section is the literature review; the third section presents the research methods; the fourth section provides a detailed introduction to the case region and data sources; the fifth section presents the assessment results; the sixth section analyses and discusses the results; and the final section presents the conclusion.

2. Literature review

Resilience means "the ability to recover from some disturbance", which originates from the Latin word "resilio" (Cimellaro et al., 2010). It is widely believed that resilience is the ability of a system to re-establish normal conditions after the occurrence of an event that disrupts its state (Hosseini et al., 2016). Unlike risk assessment studies that focus on identifying critical risks to a system, the resilience perspective puts more emphasis on the ability of a system to adapt and recover from shocks (Longbin and Hanping, 2024). The proposal of resilience offers a new research perspective for systems to withstand unpredictable risks. However, resilience assessment research on subway system to waterlogging disaster still needs more efforts. Goldbeck et al. (2019) developed a dynamic network flow models to assess the resilience of London's subway to a local flooding incident. Nishant et al. (2020) developed a hypothesis-driven resilience framework based on complex network theory to assess the resilience of the London rail network under intense flood hazards exacerbated by targeted attacks. Zhou et al. (2021) utilized the meteorological warning signals and ridership resilience curve to analyze the resilience of subway ridership under extreme rainfall. Gao et al. (2024) assessed the resilience of road segments near subway stations resilience during rainfall disturbance through link reliability and further quantified the system resilience based on segment failure and recovery probabilities. Prevailing studies have predominantly concentrated on risk assessment. For instance, Wang et al. (2021a) assessed flood risk of subway system in Guangzhou using improved trapezoidal fuzzy analytic hierarchy process (AHP). Zheng et al. (2022) proposed an integrated approach to assess the risk of rail traffic system flooding disaster during Zhengzhou "7.20 Storm". Lyu et al. (2020) built a flood risk assessment structure of Shenzhen subway system, including precipitation, natural environment, population density, and so on, from dimension of hazard, exposure, and vulnerability. These studies on waterlogging resilience or risk assessment of subway system seldom incorporate hydrological models to characterize real inundation situations and often neglect the influence of subway system characteristics on the incidence of waterlogging.

The index comprehensive assessment methodology is the most commonly used method in resilience assessment, which uses several key indexes to describe the characteristics of a system (Kotzee and Reyers, 2016; Yang et al., 2023). The research objects are assessed based on the information provided by various indexes, so that researchers can make both horizontal and vertical comparisons among the subjects. Existing resilience assessment of subway system to waterlogging typically consider factors including the subway system's engineering facilities, the subway station's external environment, external resources, emergency equipment and emergency plans. selected 20 indexes, including type of exit, resident population, medical, and emergency response capabilities, to evaluate the resilience levels of 13 subway stations in Chongqing against rainstorms. However, these indexes cannot adequately capture the unique challenges subway systems face during waterlogging events, such as the difficulty in braking subway trains, high passenger flow at interchange stations, an enclosed internal environment, circuitous escape routes, and the complexities associated with passenger evacuation, all of which can make the subway system more vulnerable to waterlogging. Moreover, rainfall events are often employed as a trigger for waterlogging (Lyu et al., 2019a, 2019b; Lyu et al., 2018, 2020; Xiao et al., 2023). However, merely considering rainfall events is insufficient to reflect the spatial distribution pattern of surface drainage situation in the study area. Instead, applying a hydrological model can more accurately reflect the surface drainage situation (Lyu et al., 2019). The InfoWorks ICM model can completely simulate the urban rainwater cycle and illustrate the interactions between the urban drainage network system and the surface water body (Yang et al., 2023). Accordingly, we expand the scope of assessment by incorporating subway unique characteristics as additional key indexes, such as the number of subway route, departure interval time, station length and subway supporting facilities, and using the simulation results of waterlogging (inundation range, inundation depth, and inundation duration) as the judgment of surface water accumulation. Based on these factors, a comprehensive assessment index system of SSWR is proposed.

Although the index comprehensive assessment methodology can highlight the factors influencing resilience, it cannot describe the dynamic changes and balance of system performance during a disturbance event. It lacks a process-based consideration of resilience, falling to capture the evolving nature of system response(Feng and Zeng, 2024). Bruneau and Reinhorn (2007) first proposed the concept of system performance curve and applied it to the study of seismic resilience of community and infrastructure systems. Since then, this method has been widely applied to the study of resilience of other systems (Goldbeck et al., 2019; Liu et al., 2022; Ma et al., 2023; Yu et al., 2023b). With the deepening and systematization of transportation resilience study, researchers use the concept of "system performance curve" and combine the three stages of disaster (before, during, and after disaster) to build a resilience measurement index, such as robustness, vulnerability and recoverability (Zhang et al., 2024), so as to characterize the change process of system resilience under disaster disturbance. Martello et al. (2021) employed the concept of system performance to delineate the operational dynamics of Boston's rail rapid transit network through pre-disruption, disruption (response and recovery), and post-disruption phases under coastal flood events. Fang et al. (2022) divided the fluctuation of transportation system performance into four stages, including the original stability stage, disruption stage, recovery stage, and the new stable stage, in order to evaluate the resilience of transportation system under natural disasters. Despite the extensive application of system performance curves in evaluating transportation system resilience, they are not commonly used in assessing subway system resilience under waterlogging disasters. Research in this area lacks a unified framework to effectively describe the changes in system performance. Therefore, based on the system performance curves, this study proposes a "Stability-Resistance-Recovery" assessment framework in view of the three stages of waterlogging disasters (before, during, and after). Within this framework, 25 influencing indexes are identified to assess subway system waterlogging resilience and to offer practical, systematic guidance about how to assess resilience.

Several methods have been proposed for the index comprehensive assessment, such as the technique for order preference by similarity to an ideal solution (TOPSIS) (Hwang and Yoon, 1981), fuzzy evaluation (Zadeh, 1968), grey relation analysis (GRA) (Deng, 1989), and data envelopment analysis (DEA) (Charnes et al., 1978). TOPSIS ranks the evaluation object by measuring the distance between the evaluation object and the optimal solution, and the distance between the evaluation object and the worst solution. This model can fully leverage the

information in the original data, and the results can accurately reflect the gaps between the evaluation objects. Because it can obtain good comparability assessment ranking results, TOPSIS is now a well-accepted method for conducting assessments (Peng et al., 2023; Yang et al., 2020). However, the importance of different indexes varies, so that scientifically and reasonably calculating index weights can improve the rationality and credibility of assessment results. Thus, a necessary step is to determine the weight of each index when using TOPSIS (Chen, 2021). The entropy weight method (EWM) is one of the most commonly used methods for calculating weights. This method is an objective weighting method, therefore, the weights obtained from this method are more reliable and accurate than those obtained from the subjective weighting method (Zhang et al., 2022). The EWM has been verified in water quality assessment (Zhe et al., 2021), ecological assessment (Xie et al., 2018), and food quality and safety assessment (Han et al., 2023). Based on this literature review, this study introduces the EWM into the TOPSIS model to assess the SSWR.

The aims of this study are: (1) to apply a "Stability-Resistance-Recovery" framework for SSWR considering the waterlogging process; (2) to establish a comprehensive index system based on a hydrological model and characteristics of the subway system for the SSWR assessment; and (3) to analyze the spatial distribution of the SSWR in the CUAB and provide a scientific basis for disaster prevention and post-disaster restoration. The novelty of this study lies as followed: (1) to comprehensively address the waterlogging problem of subway systems, the InfoWorks ICM model was employed to simulate the interaction process of rainfall runoff, drainage pipe confluence, and surface water. This approach allows for a detailed consideration of the interactions between the subway station and its surrounding environment. By using model simulation results, including inundation range, inundation depth, and inundation duration, instead of relying solely on a single rainfall event as the cause of waterlogging, we can obtain a more accurate assessment results of waterlogging resilience; (2) several indexes were defined and quantified to describe the unique characteristics of subway systems compared to surface transportation systems. It constructed a more comprehensive assessment index system for assessing the SSWR, offering a novel approach for the selection and calculation of assessment indexes.

3. Methodology

3.1. Framework for SSWR assessment

The level of resilience depends on the performance of the system from being destroyed to recovery. To analyze the resilience of the subway system in the face of waterlogging disturbance, the first step is to describe the whole response process of the system while being damaged. Resilience is a manifestation of a process, which can be regarded as a process responding to and recovering from waterlogging. The three distinct stages of waterlogging (pre-, during, and post-disruption) align with three specific dimensions of resilience. These dimensions encompass a range of abilities that collectively contribute to the overall resilience of systems (Francis and Bekera, 2014; Martello et al., 2021; Yu et al., 2023a). Therefore, this study proposes that in the face of waterlogging interference, the subway system resilience refers to the maintaining and restoring the normal level of service, and face the next interference, that is, the organic combination of the stability, resistance, and recovery. This study takes the process of disturbance caused by heavy rainfall as the timeline, dividing the system performance state into disaster prevention stage, disaster diffusion stage, and response-recovery stage, as shown in Fig. 1. This study shows the changes of the performance level of the subway system under attack to identify the various factors that affect resilience, and builds an index system of SSWR in the dimensions (the stability, resistance, and recovery) based on the system performance curve.

The disaster prevention stage refers to the period from the occurrence of a disruptive event to the occurrence of negative impacts. A subway system is disturbed by emergencies, which is the premise of its performance abrupt change (Bruneau et al., 2003). There is a certain depth of water accumulation around the subway entrance (at time t_0-t_1) when heavy rainfall occurs, but the stability of the subway system make it maintain original equilibrium state, greatly reducing the risk of ponding into the subway entrance.

As a rainstorm continues, the negative impact begins to appear, that is, the water around the subway entrance begins to pour back into the subway interior (at time t_1). At this point, the system is in disaster diffusion stage, and a temporary closure of some entrances or a shutdown of partial stations can occur due to an abrupt reduction of performance. However, the system's resistance will absorb the negative effects of disturbances to ensure that the system's functionality is not completely damaged.

After the system performance decreases, the emergency response begins to initiate and carry out repair work (at time t_2), at which point the system is in the response-recovery stage until it returns to the original equilibrium state or another equilibrium state. In this stage, it reflects the responsiveness ability of the government, social organizations, and individuals.

3.2. Index system for the SSWR

Based on the system performance curve, a multi-dimensional index system for the SSWR is formed, which can reflect the system performance change while being attacked. Fig. S1 shows the simplified sketch of subway system threatened by rainstorm, which depicts the construction of the index system based on four aspects: 1) inundation situation, 2) natural environment, 3) subway information, and 4) sociodemographic information. Table 1 presents the selection of 25 second-level indexes, with their attribution to resilience classified as either "+" or "-", denoting the positive or negative correlation with resilience, respectively.

The factors that affect system's stability include two aspects. On the one hand, it refers to the internal or external disturbances that have a negative impact on the stability, which make the system's normal operation state susceptible to disruption (Francis and Bekera, 2014). On the other hand, it refers to factors that have a positive impact, which have the ability to maintain system's original state during the disaster prevention stage. The inundation range (IR)[1], inundation depth (IDE), and inundation duration (IDU) calculated via the InfoWorks ICM model serve as external disturbance factors, which are the premise for the system's equilibrium state being disturbed. In addition, urban development has changed the nature and structure of original land, leading to an expansion of impermeable surfaces, which significantly increases in peak runoff and flood volumes (Du et al., 2012). The hydrological conditions surrounding subway stations also influence their stability to waterlogging. Green spaces play a crucial role in mitigating rainfall runoff and minimizing the risk of waterlogging. In terms of geographical factors, elevation and slope significantly contribute to the occurrence of waterlogging disasters. Therefore, indexes, including impervious surface percentage (ISP), water body surface percentage (WSP), river proximity (RP), green space percentage (GSP), average slope (slope), and average elevation (elevation), are combined to assess the stability of the subway system.

The level of system's resistance is related to its long-term state. The construction of subway and municipal drainage pipelines directly or indirectly impacts the resistance of subway system under rainstorms, consequently affecting the resilience of the subway system. Therefore, the resistance covers eight indexes, i.e., number of exits (NE), type of exit (TE), number of subway route (NSR), morning peak departure time

[1] All nomenclatures and abbreviations in the methodology have been list in the Table S1.

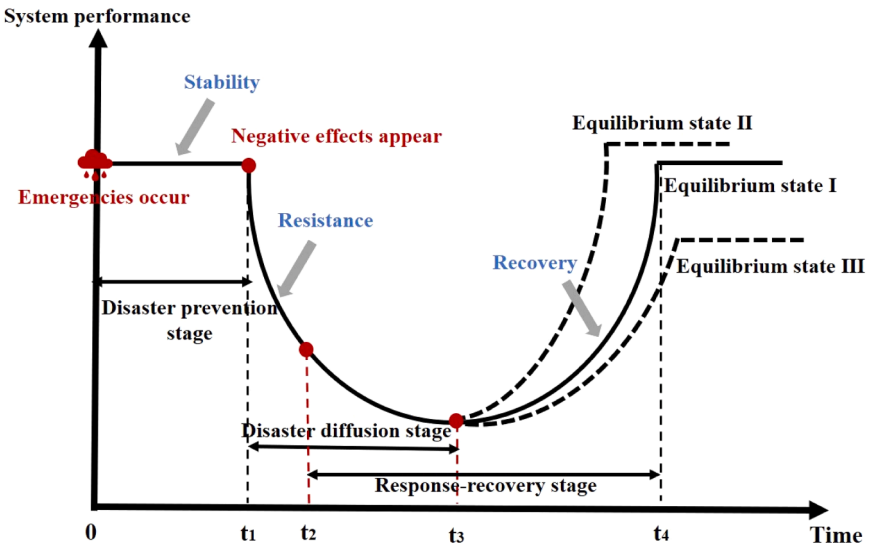

Fig. 1. The entire process of subway system being disturbed by heavy rainfall.

Table 1
The index system for the SSWR assessment based on the system performance curve.

Target layer	Disaster process	Criterion layer	Index layer	Unit	Index attribute
SSWR assessment	Disaster prevention stage	Stability	Inundation range (IR)	m^2	-
			Inundation depth (IDE)	m	-
			Inundation duration (IDU)	min	-
			Impervious surface percentage (ISP)	%	-
			Water body surface percentage (WSP)	%	+
			River proximity (RP)	m	+
			Green space percentage (GSP)	%	+
			Average slope (slope)	°	-
			Average elevation (elevation)	m	+
	Destruction diffusion stage	Resistance	Number of exits (NE)	-	+
			Type of exit (TE)	-	+
			Number of subway route (NSR)	-	-
			Morning peak departure time interval (MDTI)	min	+
			Evening peak departure time interval (EDTI)	min	+
			Station length (SL)	m	+
			Subway supporting facilities (SSF)	-	+
			Drainage pipeline density (DPD)	-	+
	Response and recovery stage	Recovery	Professional staffing (PS)	-	+
			Fire service coverage (FSC)	-	+
			Ambulance service coverage (ASC)	-	+
			Distance to hospital (DH)	m	-
			Station passenger flow (SPF)	-	-
			Population density (PD)	-	-
			Vulnerable groups percentage (VGP)	-	-
			Vulnerable facility coverage (VFC)	-	-

Inundation situation | Natural environment | Subway information | Sociodemographic information

Note: Inundation situation, natural environment, subway information, and sociodemographic information are shown in blue, orange, yellow, and green, respectively.

interval (MDTI), evening peak departure time interval (EDTI), station length (SL), subway supporting facilities (SSF), and drainage pipeline density (DPD), which are related to underground structures and infrastructure.

The recovery is related to the implementation of emergency response measures, as well as the availability and spatial allocation of emergency resources, which are the critical factors in reducing losses under extreme rainfall conditions (Yang et al., 2023). The fire and rescue services and the ambulance are the primary emergency responders to extreme flooding events (Zhang et al., 2022). Medical condition is also an important factor in disaster recovery. In addition, professional staffing (PS) also plays an undeniable role in emergency response and is selected as an index. Public awareness and ability to withstand waterlogging events are related to age, vulnerable groups such as elderly and children are severely affected by emergencies (Ekmekcioğlu et al., 2022; Lin et al., 2018). Moreover, station passenger flow (SPF) and population density (PD) (Santos et al., 2020) are typical demographic indexes for assessment. Facilities with high concentrations of vulnerable people (kindergarten, primary school, and nursing home) within the service scope of subway stations are also supposed to be taken into consideration (Yu et al., 2020).

3.3. EWM-TOPSIS

3.3.1. EWM

The EWM was introduced by Shannon in 1948 (Shannon, 1948), which is a method that utilizes the amount of information provided by the entropy value to calculate the weights of indexes (Jiao et al., 2023).

The procedure for calculation is shown as follows.

(1) Construct the original evaluation index matrix.

Assuming that there are m evaluation objects and n indexes, the original matrix (X) can be presented as follows:

$$X = \begin{bmatrix} x_{11} & \cdots & x_{1n} \\ \vdots & \ddots & \vdots \\ x_{m1} & \cdots & x_{mn} \end{bmatrix} = (x_{ij})_{mn} \tag{1}$$

where x_{ij} is the original data value of the i-th evaluation object under the j-th index.

(2) Standardize the original data of all the indexes

The evaluation indexes can be divided into positive indexes and negative indexes in the comprehensive assessment. The extremum method is used for index preprocessing to normalize the indexes and eliminate dimension.

The positive indexes are standardized as follows:

$$z_{ij} = \frac{x_{ij} - min(x_j)}{max(x_j) - min(x_j)} \tag{2}$$

The negative indexes are standardized as follows:

$$z_{ij} = \frac{max(x_j) - x_{ij}}{max(x_j) - min(x_j)} \tag{3}$$

where $min(x_j)$ is the minimum value of the j-th index, $max(x_j)$ is the maximum value of the j-th index, and z_{ij} is the standardized value of x_{ij}.

(3) Calculate the proportion of each index

$$P_{ij} = \frac{z_{ij}}{\sum_{i=1}^{m} z_{ij}} \tag{4}$$

where $i = 1,2,3,\ldots,m;\ j = 1,2,3,\ldots,n$

(4) Calculate the information entropy of each index

The larger the difference in the values of the objects on a certain index is, the smaller the entropy is, the more information it provides, which means that the index deserves a higher weight. In contrary, a smaller difference means bigger entropy, representing a lower weight. That is to say, the greater the weight is, the greater the role it can play in the SSWR assessment. The entropy of each index should be calculated as follows:

$$E_j = -\frac{1}{ln(m)} \cdot \sum_{i=1}^{m} P_{ij} \cdot lnP_{ij} \tag{5}$$

where m is the number of the objects

(5) Calculate the weight of each index

$$W_j = \frac{1 - E_j}{\sum_{j=1}^{n} (1 - E_j)} \tag{6}$$

where n is the number of the indexes

(6) Calculate the weights of the first-level indexes

Calculate the weight of 25 second-level indexes as a whole, with the weights of the first-level indexes being equivalent to the sum of the weights of the second-level indexes it contains.

3.3.2. TOPSIS

The TOPSIS model was initially proposed by Hwang and Yoon in 1981 (Hwang and Yoon, 1981) according to the closeness of the existing evaluation object and the idealized target (Xiao et al., 2023), which is a commonly used comprehensive assessment method.

The main calculation steps are as follows:

(1) Use the standardized matrix (Z) obtained from the EWM for the following calculations

$$Z = \begin{bmatrix} z_{11} & \cdots & z_{1n} \\ \vdots & \ddots & \vdots \\ z_{m1} & \cdots & z_{mn} \end{bmatrix} = (z_{ij})_{mn} \tag{7}$$

where z_{ij} is the standardized data value of the i-th object under the j-th index.

(2) Determine the optimal solution (z_{max}) and the worst solution (z_{min})

Because all the indexes are converted into optimal indexes, the optimal solution is composed of the maximum value of each index, while the worst solution is composed of the minimum value of each index.

$$z_{max} = (max\{z_{11}, z_{21}, \ldots, z_{m1}\}, max\{z_{12}, z_{22}, \ldots, z_{m2}\} \ldots, max\{z_{1n}, z_{2n}, \ldots, z_{mn}\}) \tag{8}$$

$$z_{min} = (min\{z_{11}, z_{21}, \ldots, z_{m1}\}, min\{z_{12}, z_{22}, \ldots, z_{m2}\} \ldots, min\{z_{1n}, z_{2n}, \ldots, z_{mn}\}) \tag{9}$$

(3) Calculate the weighted Euclidean distance between the i-th object and the optimal solution (d_{i_max}), and the distance between the i-th object and the worst solution (d_{i_min}).

$$d_{i\_max} = \sqrt{\sum_{j=1}^{n} W_j \left(z_{max} - z_{ij}\right)^2} \tag{10}$$

$$d_{i\_min} = \sqrt{\sum_{j=1}^{n} W_j \left(z_{min} - z_{ij}\right)^2} \tag{11}$$

where W_j is the weight of the j-th index obtained from EWM, $i = 1,2,3,\ldots,m;\ j = 1,2,3,\ldots,n$

(4) Calculate the relative closeness to the optimal solution

The relative closeness, which is the assessment score (S_i) of the i-th object, can be calculated by using equation (12). The larger the score is, the better the assessment results; otherwise, and vice versa.

$$S_i = \frac{d_{i\_min}}{d_{i\_min} + d_{i\_max}} \tag{12}$$

(5) Calculate the SSWR

Therefore, the formula for calculating the SSWR is as follows:

$$SSWR = W_{sta} \cdot Sta + W_{res} \cdot Res + W_{rec} \cdot Rec \tag{13}$$

where *Sta*, *Res*, and *Rec* are the relative closeness of the stability, resistance, and recovery to the optimal solution, respectively. W_{sta}, W_{res}, and W_{rec} are the weights of the stability, resistance, and recovery, respectively.

4. Case study

4.1. Study area

Beijing, located in northern China, occupies an area of 16,410 km^2 and serves as the center of politics, culture, international exchanges, and technological innovation of China. At the end of 2022, the Beijing's resident population has reached 21,834,000, with a gross domestic product (GDP) of 3031.73 billion RMB (Chinese yuan). In the terms of land use type (Fig. S2), green space (including tree, shrubland, and grassland) occupies more than half of the total area of Beijing, accounting for 61.31%. The built-up area (including buildings and roads) accounts for 15.42%, and water bodies occupy 1.55%. In the remaining areas, cropland, bare land, and wetland accounted for 18.06%, 3.61%, and 0.04%, respectively. Beijing is situated in the warm temperate semi-humid and semi-arid monsoon climate zone. The average annual temperature is 13.6°C, and the average annual precipitation is 698.4 mm, approximately 75.89% of which occurs from July to September (National Bureau of Statistics of China, 2022). Under such climate conditions makes Beijing vulnerable to waterlogging (Wang et al., 2020).

24 subway lines were in operation in Beijing (Fig. S2), with approximately 760 km and 427 stations by July 1, 2023. The average daily passenger flow of the Beijing's subway stood at approximately 9 million in the first half of 2023, with a peak reaching 13.8 million in a single day (https://metrodb.org). Thus, the Beijing subway system is among the busiest subway systems in China. Because of the rapid urban development (Lyu et al., 2019a), the complexity of subway network structures (Lyu et al., 2020), extreme rainfall (Forero-Ortiz et al., 2020), and land subsidence (Wang et al., 2021b), subway stations are one of the vulnerable structures that are exposed in flood-prone areas.

It can be seen from Fig. S2 that due to the influence of urban construction, the central region of Beijing is extensively covered with impermeable surfaces such as buildings and roads, with less distribution of green spaces and water bodies, making this area more prone to surface waterlogging. Moreover, this area is the core region of Beijing's urban development, hosting approximately 69% of the subway stations, with intensive human activities. Therefore, this study selected the central urban area of Beijing (CUAB) as the study area (Fig. S3) and construct the Beijing waterlogging model based on it. The CUAB is located in the northeastern part of the North China Plain, where the Yongding River passes to the southwest. The study area includes two capital functional core areas (Dongcheng District and Xicheng District), and parts of four urban functional expansion areas (Chaoyang District, Haidian District, Fengtai District, and Shijingshan District).

4.2. Data collection and processing

4.2.1. Inundation situation

This study utilized InfoWorks ICM to comprehensively consider processes such as rainfall runoff, pipe network convergence, and surface water flooding, and used high-precision DEM data to divide 2D triangular mesh, to simulate the inundation depth, duration, and range of each 2D triangular mesh under rainstorm with a return period of 50 years for Beijing. The Code for Design of Subway (GB50157) stipulates that the entrance and exit of subway stations should be 30-45 cm above the outdoor ground, thus, the areas with a depth of inundation greater than 30 cm are extracted by the ArcGIS platform. When the depth of accumulated water exceeds this depth, there is a risk of water ingress into the subway. A detailed list of the datasets, along with the source and resolution of the data, is shown in Table 2.

The research selects 181 subway stations on 21 subway lines in the CUAB, and extracts the triangular mesh which the depth of accumulated water is greater than 30 cm within a 100-meter buffer zone based on the subway station. The inundation depth and time in different triangular meshes are different, thus, this study obtains the IDE and IDU within the buffer zone according to the IR of each grid. The formulas for calculating the IDE and IDU are as follows:

$$IDE = \sum_{i=0}^{c} \frac{R_j E_j}{\sum_{i=0}^{c} R_i} \tag{14}$$

$$IDU = \sum_{i=0}^{c} \frac{R_j U_j}{\sum_{i=0}^{c} R_i} \tag{15}$$

where R, E, and U are the inundation range, depth, and duration of the grid respectively, c is the number of triangular meshes contained in the buffer, and $0 \ll j \ll i \ll c$.

4.2.2. Natural environment

Fig. S4 shows the spatial distribution of Land use land cover (LULC) and topography in the CUAB. The built-up and water bodies are extracted separately from LULC to calculate the ISP and WSP within a 500-meter buffer zone based on the subway station, whereas the river proximity (RP) refers to the distance between the subway station and the closest river. Urban green space (UGS), one of the most important components of the urban ecosystem, refers to vegetation entities in the urban area, such as parks and green buffers (Shi et al., 2023), so that the study uses UGS dataset to calculate the GSP, which is defined as the ratio of the area of green space within a 500-meter buffer zone of the station to the area of the zone. The slope and elevation are calculated with a digital elevation model (DEM) in ArcGIS 10.5. The central region has a total higher slope than the other regions, while the elevation shows a decreasing pattern from the west to the east.

4.2.3. Subway information

The basic information of the subway is shown in Fig. S5. The NSR

Table 2
The data used in this study.

Category	Data	Source	Resolution
Remote sensing images	Landsat8 (2021)	https://www.gscloud.cn/	30 m
Simulation of urban waterlogging	Inundation range	Simulated in the study	–
	Inundation depth	Simulated in the study	–
	Inundation duration	Simulated in the study	–
Land use land cover	LULC (2020)	https://esa-worldcover.org/en	10 m
River system data	River (2023)	https://www.openstreetmap.org/	–
Urban green space	UGS (2023)	https://www.scidb.cn/en	1 m
Topography	DEM	https://www.gscloud.cn/	12.5
Subway information	Number of exits	https://www.bjsubway.com/	–
	Type of exit	maps.bimw.cn/baidujiejing/	–
	Number of subway route	https://www.bjsubway.com/	–
	Train timetable	https://www.bjsubway.com/	–
	Station length	Collected in the study	–
	Subway supporting facilities	https://www.bjsubway.com/	–
	Drainage pipeline system	http://www.iwhr.com/zgskywwnew/index.htm	–
	Professional staffing	https://www.bjsubway.com/	–
	Station passenger flow (2016)	https://gda.bnu.edu.cn/sypt/sjgx/csyjsjj/index.html	–
Sociodemographic information	Fire station (2021)	https://www.resdc.cn/	–
	Emergency Center Station (2021)	https://www.resdc.cn/	–
	Hospital (2021)	https://www.resdc.cn/	–
	Population (2020)	https://www.worldpop.org/	100 m
	Age and sex structures (2020)	https://www.worldpop.org/	100 m
	Care home, primary school, and kindergarten (2020)	https://www.resdc.cn/	–

represents whether a subway station is an interchange station or not, and how many subway lines pass through the station. The SSF includes AED and emergency calling device. The PS of the subway is replaced by the number of police offices and comprehensive control offices. There are four types of subway exits, namely open, enclosed, semi-enclosed, and concealed (Fig. S6). Over 700 images are extracted from Baidu Street View (maps.bimw.cn/baidujiejing/), and manual visual interpretation is used to determine the type of subway station exit. This study quantifies the TE through the assignment method, with numbers 1, 2, 3, and 4 representing open, semi-closed, closed, and concealed forms, respectively. When there are multiple different types of exits in a subway station, the average score represents the exit type. The morning peak (7:00-9:00) and evening peak (17:00-19:00) hours are selected as the research periods when calculating the departure time interval. The MDTI and EDTI originate from the train timetable (https://www.bjsubway.com/). To reflect the intraday changes during normal working days, the weekday schedule is selected for calculation.

The SPF refers to the total number of people entering and exiting a subway station over a period of time. This study selects approximately 140 million card swiping data from five working days (June 1st, 2nd, 3rd, 6th, 7th) in 2016 for research. The traffic network data (Zhao et al., 2020) are supported by the Center for Geodata and Analysis, Faculty of Geographical Science, Beijing Normal University (https://gda.bnu.edu.cn/sypt/sjgx/csyjsjj/index.html). The study calculates the average number of people entering and exiting the subway stations per hour during morning and evening peak hours as the passenger flow.

This study collects and organizes the urban drainage network for the research area, reasonably simplifies it, and removes the sewage pipelines, resulting in a simplified network with a total length of approximately 2,229 km. As shown in Fig. S7, the network density is higher within the Third Ring Road and lower outside the Fourth Ring Road. The simplified drainage network data is applied to the InfoWorks ICM model to simulate the actual water collection process of the network. This approach allows for an accurate simulation of surface water accumulation, providing precise waterlogging results and reflecting the drainage capacity near subway stations to some extent. In addition, the DPD is defined as the ratio of the total length of pipelines within a 500-meter buffer zone of the subway to the area of the zone. We incorporate the DPD as an independent index in the assessment index system to assess the subway system's resistance to waterlogging.

4.2.4. Sociodemographic information

In this study, a 5-kilometer buffer zone within each fire station is established as the service area, and the number of times that each subway station is covered by the buffer zone are represented as the FSC of the subway station. The calculation method of the ASC is the same as that of the FSC. In addition, the DH refers to the distance between the subway station and the closest hospital (Xiao et al., 2023).

The PD and VGP refer to the data within the 500-meter buffer of the subway station, where vulnerable groups refer to the people under 10 years old and over 60 years old. Moreover, the VFC refers to the total number of kindergartens, primary schools, and nursing homes inside the buffer zone.

5. Results

5.1. The results of waterlogging risk

The areas with inundation depths exceeding 30 cm were identified and extracted via the waterlogging simulation results. Subsequently, the waterlogging risk value was simulated by multiplying the range, depth, and duration of inundation. These values were categorized into five levels employing a natural discontinuity method. Fig. 2 displayed the spatial distribution of waterlogging risk levels. The higher waterlogging risk was primarily concentrated in the central and southern regions, mainly distributed in the northern part of Dongcheng District and Xicheng District, the southern part of Haidian District, and the eastern part of Fengtai District. Subway stations that are located in close proximity to high waterlogging risk areas, such as Hepingman Station, Qianmen Station, and Wangfujing Station, are predominantly situated along subway lines 1, 2, 10, and 14.

5.2. Weights of the resilience assessment indexes

Table S1 showed the weights of each index calculated using EWM. In general, a higher weight of indicates a greater impact on resilience. Both the stability (0.4712) and resistance (0.3517) were about twice the influence on the SSWR compared to the recovery (0.1771). From the perspective of stability, the LULC around the subway station had a significant impact, especially the distribution of water bodies and rivers, while the influence of topography was relatively minor. This means that the significant influence of the natural environment surrounding subway stations in maintaining stable operations of the stations during waterlogging. From the perspective of resistance, the time interval of departure, number of exits, station length, and the distribution of

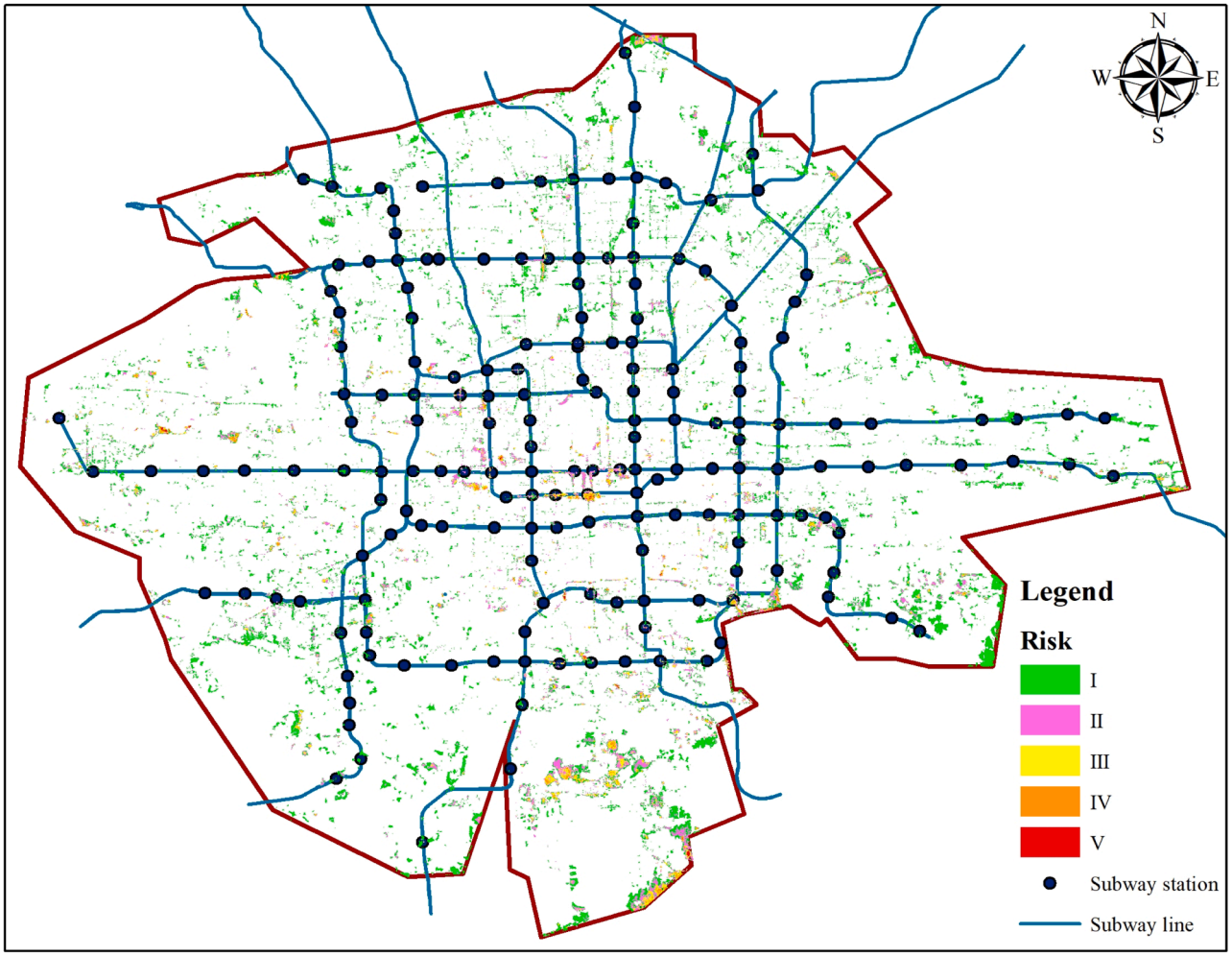

Fig. 2. Spatial distribution of waterlogging risk levels.

drainage pipeline exerted strong driving forces on resistance. From the perspective of recovery, the distribution of emergency response resources and population was the key factors influencing the recovery. This highlights the importance of rationally allocating emergency resources for disaster recovery. Population density exhibits an inversely proportional to the recovery to waterlogging, because densely populated areas face higher risks and pose greater challenges for rescue operations. Although vulnerable groups and station passenger flow could also have a negative impact on the recovery, their influence was not as pronounced as that of the aforementioned indexes.

5.3. The assessment results in different dimensions of SSWR

The stability, resistance, and recovery assessment results for each subway station were categorized into five levels using the natural discontinuity method. Levels I, II, III, IV, and V represented very low, low, medium, high, and very high, respectively. A higher score indicates that the system performance is better in the process of responding to and recovering from waterlogging. The station quantity of the stability, resistance, recovery, and SSWR in five level were shown in Table 3.

The stability was classified into five levels: I (0.117~0.185), II (0.185~0.230), III (0.230~0.286), IV (0.286~0.386), and V (0.386~0.716). As illustrated in Table 3, only 17.7% of subway stations reached a very high or high stability level, while 23.1% attained a medium level, leaving more than half of the subway stations at a very low or low stability level. The spatial distribution of the stability in the CUAB was depicted in Fig. 3 (a). Subway stations at very low or low stability levels were predominantly concentrated in the central area, which was consistent with the outcomes of the waterlogging risk assessment. The stability of subway stations in the northwest surpassed that in other regions, with a majority of them situated along subway lines 1, 4, and 10. Furthermore, the stations at the medium level of the stability featured the most extensive areas.

Table 3
Station quantity of stability, resistance, recovery, and SSWR in five level.

Level	Quantity of subway			
	Stability	Resistance	Recovery	SSWR
I	25	51	20	28
II	75	66	47	66
III	49	45	51	59
IV	26	13	42	22
V	6	6	21	6

The resistance was classified into five levels: I (0.188~0.267), II (0.267~0.322), III (0.322~0.401), IV (0.401~0.535), and V (0.535~0.682). Similar to stability, the resistance of the subway system generally exhibited very low or low levels. 64.6% of subway stations displayed very low or low resistance levels, while only 10.5% of stations exhibited very high or high resistance. The spatial distribution of the resistance in the CUAB was presented in Fig. 3 (b). Obviously, the resistance levels showed a decreasing pattern from the central area towards the outer periphery. Stations at very low or low resistance were mainly concentrated on subway lines 1, 2, 4, 5, 6, 9, and 10.

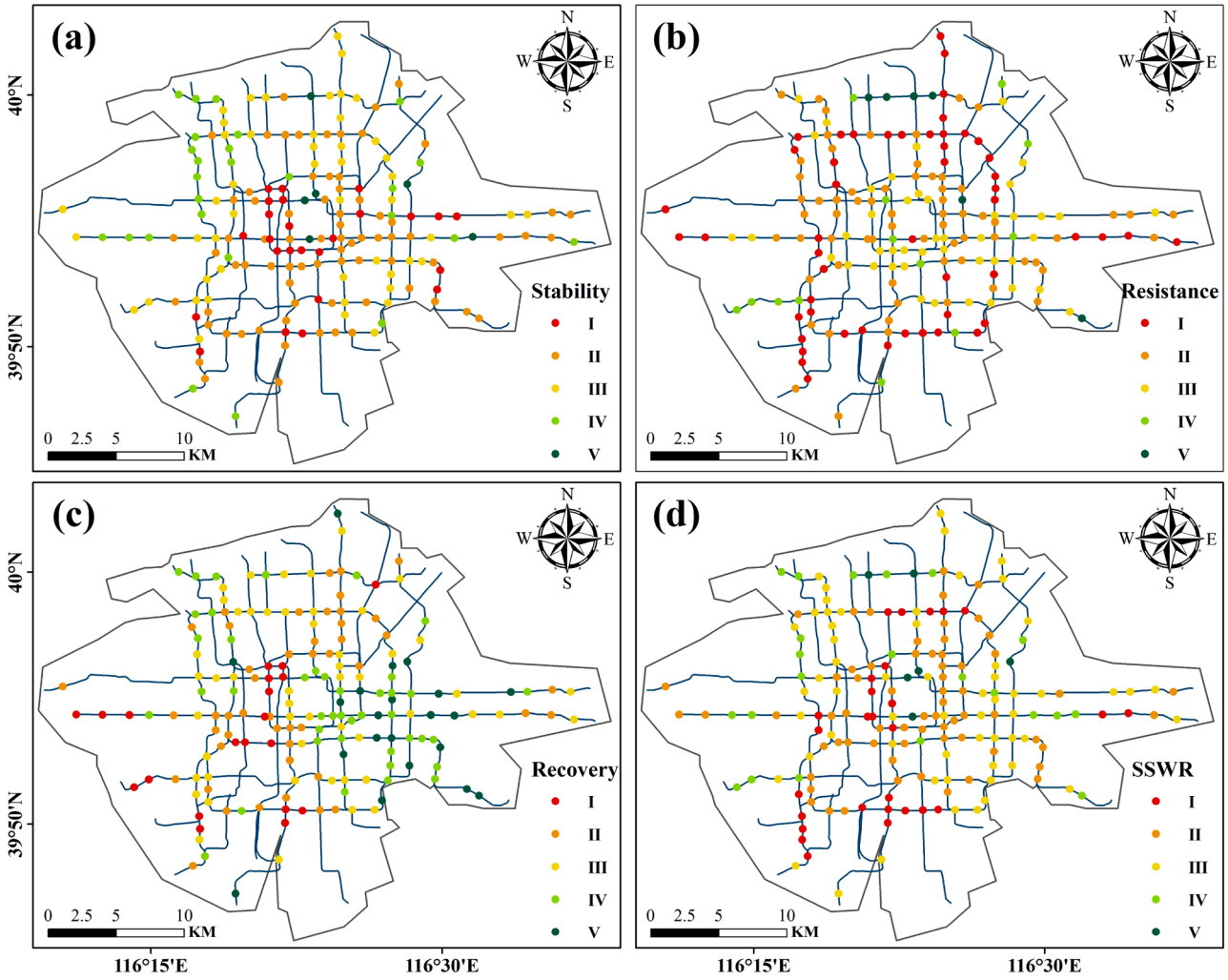

Fig. 3. Spatial distribution of the stability (a), resistance (b), recovery (c), and SSWR (d) in the CUAB.

The recovery was classified into five levels: I (0.320~0.374), II (0.374~0.423), III (0.423~0.465), IV (0.465~0.512), and V (0.512~0.588). As shown in Table 3, 34.8% of subway stations demonstrated a very high or high level of the recovery, whereas only 11.1% of subway stations exhibited a very low level of recovery. In comparison to the system's stability and resistance, the recovery value of subway system was relatively high on the whole, which proved its relative advantage in disaster recovery. Fig. 3 (c) showed a significant regional difference of the recovery in the CUAB, with a high level observed in the eastern region and a low level in the western region. Specifically, stations at very high or high recovery levels were primarily concentrated on subway lines 1, 6, 7, and 10 in Dongcheng and Chaoyang Districts. Stations at very low and low recovery levels were mainly situated in Fengtai and Xicheng Districts, while stations at a medium recovery level exhibited a scattered distribution pattern throughout the CUAB.

5.4. The assessment results of SSWR

The subway system generally exhibited a relatively low level of resilience to waterlogging, which was classified into five levels: I (0.215~0.263), II (0.263~0.298), III (0.298~0.334), IV (0.334~0.406), and V (0.406~0.566). It can be seen from Table 3 that 51.9% of subway stations exhibited a very low or low level of SSWR, while only 15.5% had a very high or high level of SSWR. Fig. 3 (d) mapped the spatial distribution of the SSWR. The subway stations at very low or low SSWR were primarily located on subway Line 10, accounting for 26.6% of the stations falling into these categories. The remaining stations were primarily found on lines 1, 2, 4, 5, 7, and 9. Stations at a medium SSWR level were dispersed throughout areas neighboring the very low and low SSWR stations, mainly on lines 4, 6, 10, and 14. Moreover, the number of stations at a very high or high SSWR was very small, and these stations were mainly scattered in peripheral areas.

As shown in Fig. 4, comparing the number of subway stations at different levels of the stability, resistance, recovery, and SSWR on each subway line, it was found that the subway system excelled primarily in the response-recovery stage. Taking Line 10 as a case in point, 33.3% of subway stations showed a very high or high level of the recovery, while only 22.2% and 11.1% of subway stations were at a very high or high level of the stability and resistance, respectively. In particular, Lines 8 and 14 stood out for their superior SSWR performance, characterized by fewer subway stations at very low or low SSWR, with the majority registering at a medium or higher SSWR level. Nevertheless, the SSWR level of the remaining lines was relatively low, especially for Line 2, where 88.8% of subway stations were at very low or low levels of the SSWR.

The performance of subway stations when facing waterlogging was illustrated in the scatter plots (Fig. 5), which compared the SSWR to the resilience in three dimensions (the stability, resistance, and recovery) for the 181 subway stations. The top three subway stations in terms of the SSWR were Olympic Park Station (0.5658), Beihaibei Station

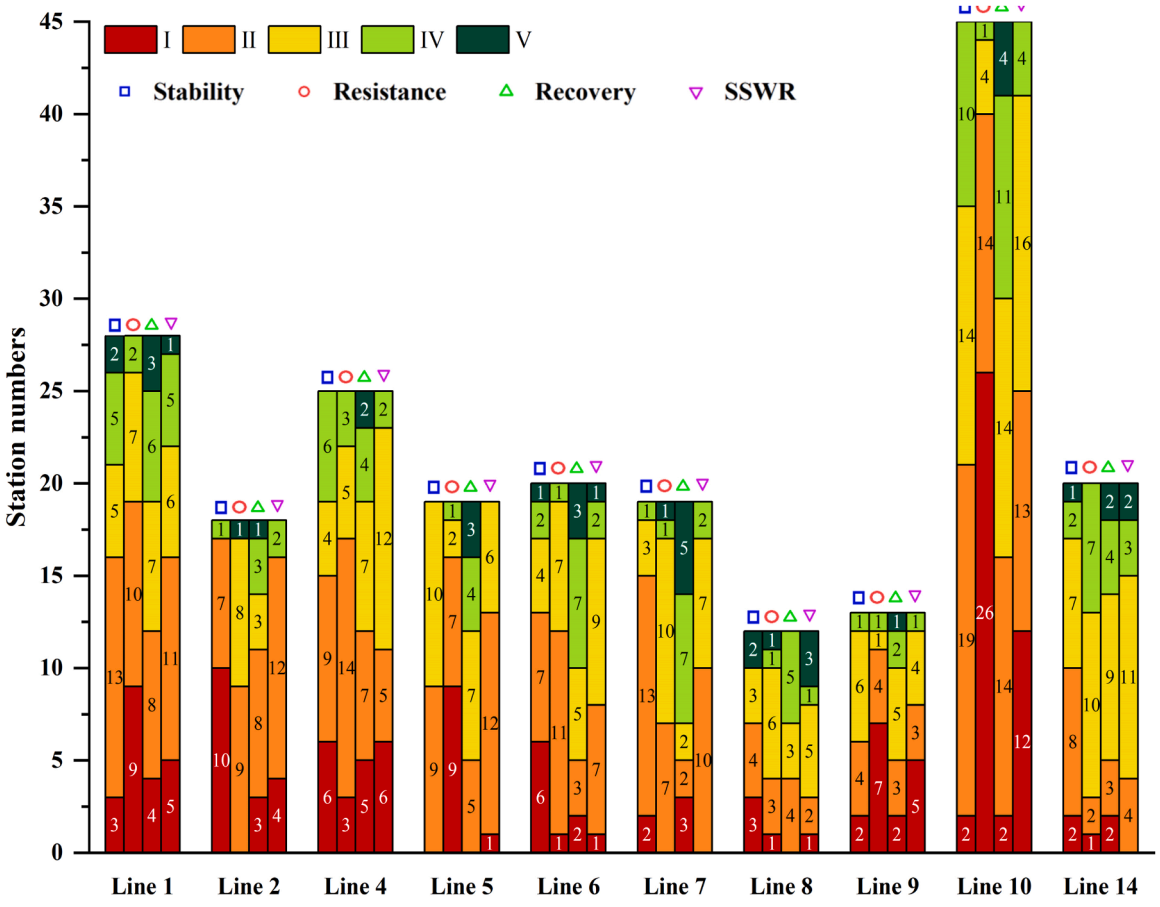

Fig. 4. Station numbers of the stability, resistance, recovery, and SSWR in five levels on each subway line.

(0.5394), and Tiananmenxi Station (0.4643), while the lowest three were Jiaomendong Station (0.2154), Keyilu Station (0.2338), and Huixinxijienankou Station (0.2348). Overall, the subway system performed relatively well during the response-recovery stage. Specifically, 92.8% of subway stations had SSWR values less than 0.375, with superior performance of the recovery. 4.4% of subway stations had SSWR values ranging from 0.375 to 0.433, with stronger resistance compared to the stability and recovery. The remaining 2.8% of subway stations mostly displayed the strongest stability. It is evident that the dispersion of the stability was the most pronounced, while recovery showed minimal dispersion, indicating significant differences in performance among subway stations during the disaster prevention stage. Remarkably, subway stations with higher SSWR values actually exhibited superior stability, suggesting their superior ability to maintain stability in the early stage of waterlogging. Conversely, subway stations with lower SSWR values often excelled in recovery, indicating their superior performance during the post-disruption phase.

6. Discussion

6.1. Analysis of the index system for the SSWR

6.1.1. Stability

It is widely believed that the inundation situation, land use type, and topography in the vicinity of the subway system can all affect its stability. In fact, subway stations at very low or low stability levels exhibit certain common characteristics, that is, these stations are located in close proximity to rivers, and have small water bodies area and green space area within a 500-meter radius of each subway station, whereas impermeable areas are large.

Extreme precipitation is the direct cause of waterlogging in subway systems. Previous studies often use assessment indexes such as storm intensity and annual average rainfall to analyze the impact of extreme rainfall on the risk of subway waterlogging (Lyu et al., 2019b; Lyu et al., 2020; Zheng et al., 2022). In these studies, the precipitation typically holds a significant weight in the index system. In contrast, we used the results simulated by the InfoWorks ICM model (inundation range, depth, and duration) as direct driving factors for subway waterlogging. Interestingly, these indexes have a relatively low weight. It is supposed that the main reason is that the hydrological model, when simulating urban waterlogging, comprehensively considers the interaction processes of rainfall runoff, drainage pipe confluence, and surface water. Consequently, its results are often closer to the actual surface waterlogging situation than those considering precipitation alone. The inclusion of drainage facilities, which mitigate waterlogging, could be the primary reason for the lower weight of these indexes.

As illustrated in Fig. S4 (a) and (c), a high concentration of buildings and roads in the central area of the CUAB was accompanied by a comparatively limited extent of green space coverage. Most subway stations located in this region exhibit lower levels of the stability, as exemplified by Xuanwu Men Station and Xisi Station. This shed light on the significant influence of land use types on waterlogging resilience assessment, which tie well with the findings of previous research (Liu et al., 2023; Yolina et al., 2023). Reasonable planning of green space in urban area can enhance the stability. Recently, the utilization of green space to bolster the stability has become increasingly prevalent, as green land plays a crucial role in mitigating stormwater runoff by intercepting rainfall and enhancing infiltration (Kuehler et al., 2017). Areas with high waterlogging risk are mainly clustered in highly urbanized areas (Zheng and Huang, 2023). This is primarily due to the expansion of impermeable surfaces (Jin et al., 2024), such as built-up areas and roads, which have a negative impact on enhancing the stability (Feng et al.,

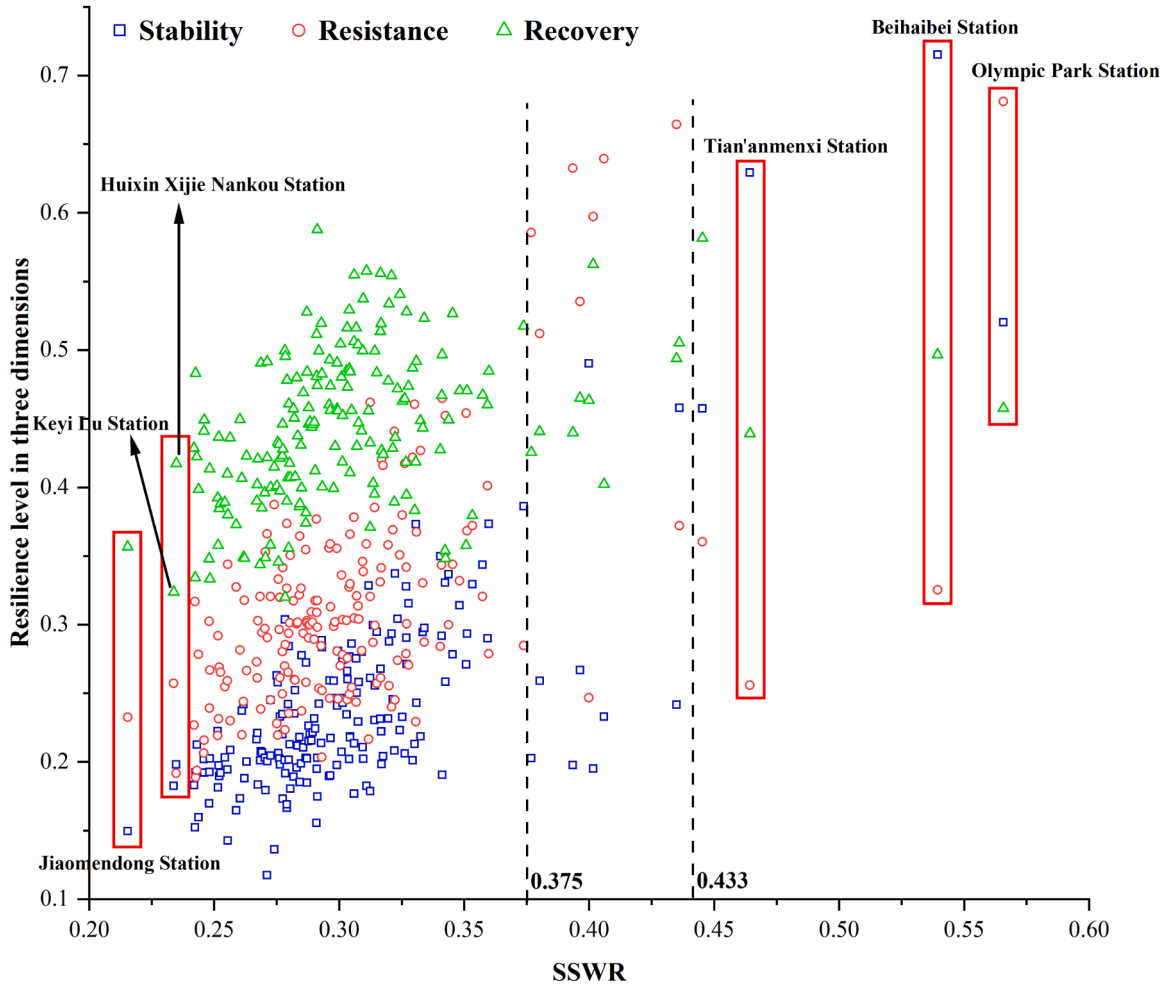

Fig. 5. Scatter plots of SSWR versus resilience level in three dimensions (stability, resistance, and recovery).

2021). Permeable surfaces have been replaced with impervious materials, which has resulted in a reduction in the surface infiltration rate and city's drainage capacity (Du et al., 2015; Jr and Gibbons, 1996). This alteration has disrupted the original water cycle process (Yang et al., 2022), increasing the risk of water accumulation and backflow. Ultimately, the resilience of subway system to waterlogging has potentially been compromised. Analogously, this also explains that subway system in many other mega-cities, such as Shanghai (Lyu et al., 2019), and Zhengzhou (Zhao et al., 2022), are also more susceptible to waterlogging due to urbanization. In addition, water bodies exhibit a dual impact on the stability. On the one hand, these water bodies act as natural reservoirs with the capacity for floodwater storage (Wu et al., 2020). On the other hand, the closer to a river, the greater the potential risk of exposure for people to waterlogging events (Ceola et al., 2014; Mård et al., 2018). For example, the stations at the lowest stability level, namely Ping'anli Station, Hepingmen Station, and Changchun Jie Station, are situated in areas where the water body surface percentage is 0 and are located too close to a river.

The topography (e.g., elevation and slope) at the entrance and exit of the subway stations also affects the diffusion of surface water accumulation. According to Fig. S4 (d) and (e), the elevation of the CUAB is higher in the northwest and lower in the southeast, while the slope of the central area is relatively steep, which corresponds to the spatial distribution of the stability levels. In other words, subway stations at low elevations and steep slopes are more prone to result in waterlogging when extreme rainstorm occurs (Lyu et al., 2018).

6.1.2. *Resistance*

The improvement of underground infrastructure is of great importance to ensure the safety of people's lives and property while disasters (Huang et al., 2022). Most subway stations at high resistance level have better subway infrastructure configurations. For example, the more the number of exits a subway station has, the higher the speed and efficiency of passenger evacuation, such as Xidan Station and Ping'anli Station. Moreover, the open exit is the most vulnerable exit type to waterlogging.

Moreover, waterlogging exerts greater pressure on the resistance of an interchange station than a regular station (Wang et al., 2021a). It can be attributed to the higher volume of passengers at interchange stations, which makes subway stations more prone to serious cascade disasters, such as stampede deaths. And interchange stations often encompass multiple transit lines, requiring more complex coordination to maintain their normal operation. Drainage systems can effectively reduce the negative effects of waterlogging (Singh et al., 2023; Sohn et al., 2020). As shown in Fig. S7, the drainage pipelines in the central area exhibit a dense distribution, resulting in relatively high level of the resistance. When the rainfall intensity exceeds the capacity of the drainage system, it will cause excessive depth of surface water accumulation to flow back into the subway stations.

In the resistance dimension, this study innovatively selected and quantified a series of indexes to characterize the unique characteristics of the subway system, including morning and evening peak departure time intervals, station length, and subway supporting facilities, which are important factors affecting the resistance, that is, these indexes of the resistance dimension played a dominant role in the SSWR. To alleviate

the frequent occurrence of uneven passenger flow and high passenger volume during peak hours of the subway, one potential solution is to increase transportation capacity, which can be achieved by compressing driving intervals. However, excessively small departure intervals cannot cope with unexpected events and delays, as they are more likely to cause train conflicts when speed limits or emergency braking are required, resulting in reduced the resistance of the subway stations, such as Jingsong Station and Tuanjiehu Station. Additionally, longer subway station provides more space for passengers, which can serve as a buffer during emergencies, reducing congestion and improving evacuation efficiency, such as Ping'anli Station and Xin'gong Station. Subway supporting facilities also play an important role in increasing system's resistance. The presence of AEDs and emergency calling devices enhances the system's ability to respond to medical emergencies and other incidents, thereby increasing the overall resilience. For example, Jiaohua Chang Station and Zhushikou Station have high resistance level, as they are equipped with a large number of AEDs and emergency calling devices. Although there are no relevant studies dealing with these indexes, traditional indexes tend to focus on structural and engineering aspects, such as drainage capacity and number of entrances and exits (Jiao et al., 2023; Wang et al., 2021a). While important, they do not fully reflect the dynamic operational characteristics and passenger management aspects that the new indexes address. The innovation indexes provide a more comprehensive view of resilience by incorporating business flexibility and emergency preparedness, providing a comprehensive assessment of a system's ability to withstand and from disruptions.

6.1.3. Recovery

In response-recovery stage, the allocation of emergency resources should be considered (Bera, 2023). Spatial planning of public resources (fire station, ambulance, hospital) plays an important role in waterlogging recovery and disparities in resources lead to regional differences in recovery. Subway stations at high recovery level have more resources to respond to waterlogging, whereas some subway stations at low recovery level are found to be more vulnerable to waterlogging and take longer to recover due to their spatial location and limited accessibility to share the resources (Kodag et al., 2022). Consequently, the accessibility of fire services and ambulance services is considered an important factor in system resilience (Coles et al., 2017; Shi et al., 2022). Moreover, the closer the incident spot is to the hospital, the better the recovery of the system after the disaster (Zhao and Zhou, 2023). And professional staffing of the subway, which is not often considered in resilience assessment, can also plays a role in maintaining order of the scene and mitigating risks to a certain extent. For example, subway stations with advantages in terms of public resources, such as Dengshikou Station and Suzhou Jie Station, exhibit strong performance in the response-recovery stage.

In addition, the larger the population density and passenger flow within the subway service area are, the higher the population pressure and passenger demand carried by the subway, which leads to a lower level of the recovery. Previous waterlogging events have demonstrated that the children and the elderly are key factors to consider, as they are more vulnerable to waterlogging compared with the general population (Cao et al., 2023; Zhu et al., 2023). Similarly, the vulnerable facility is considered to be a significant factor in assessing waterlogging resilience. These demographic indexes are related not only to individual response ability, but also to the ease of emergency rescue. For instance, Xizhimen Station and Xinjiekou Station, which are located in densely populated areas, exhibit lower recovery level.

6.2. Resilience improvement measures of subway system

The overall waterlogging risk pattern of the subway system is an important reference for urban planning and emergency response planning, which has important practical significance for flood mitigation in urban waterlogging control (Wang et al., 2021a). For subway stations near high waterlogging risk spots (Fig. 2), such as Gulou Dajie Station, it is necessary to prepare for waterlogging prevention. Meanwhile, the relevant authorities should promptly convey risk information to citizens to prevent causing casualties and property losses due to information lag.

Our research finds that a subway station at low stability level, such as Qianmen Station, has the ability to maintain normal operation during the disaster prevention stage is insufficient. Therefore, it is necessary to strengthen the construction of green infrastructure, such as setting up green space, small and medium-sized storage facilities, and improving the ecological environment.

Improving the water blocking and drainage capacity is crucial for subway stations at low resistance level. In terms of water blocking, measures such as installing roofs over fully opened subway stations, raising the height of exit steps, and incorporating intelligent water-blocking boards can be implemented, such as that seen at Huangqu Station. In terms of drainage, such as that at Guogongzhuang Station, the surrounding gray infrastructure, including drainage pipelines, pumping stations, and large-scale storage facilities, should be constructed and improved.

Emergency rescue capabilities and demographic factors can also affect the recovery of subway stations. For subway stations at low recovery level, such as Keyilu Station, it is necessary to strengthen pre-disaster education and post-disaster construction. For example, emergency drills for subway waterlogging can be conducted in collaboration with various sectors of society, including the organization and command of emergency teams, and the allocation of emergency supplies. In addition, it is imperative to provide safety education to citizens, especially to vulnerable groups, to ensure their understanding of emergency plans. Undoubtedly, this requires the joint efforts and cooperation of the government, social organizations, and individuals.

6.3. Limitations

This study assesses the resilience of subway system to waterlogging disaster and provides a new approach for the selection and calculation of indexes for future resilience assessment. However, the study still has the following limitations. Some indexes such as land subsidence, the critical soil layer (stratum) below the subway, and social inequality, etc. are not considered due to limitation of data acquisition. Furthermore, index selection is inevitably a controversial process, as scholars hold varying interpretations of the meanings and roles conveyed by diverse indexes. Therefore, when advancing index innovation, it is imperative to prioritize both comprehensiveness and objectivity.

7. Conclusions

This study established a multi-dimensional index system based on the "Stability-Resistance-Recovery" assessment framework by considering factors, such as natural environment, sociodemographic information, and unique characteristics of subway station, to analyze the SSWR under waterlogging disturbances. A case study in the CUAB showed that the stability and resistance of subway system have greater impacts than does recovery, indicating that the natural environment and characteristics of subway system have strong impacts on the SSWR. The overall SSWR in the CUAB is relatively low, especially for Line 2 and Line 10. These lines are not only located in high waterlogging risk areas, but also have a very low or low SSWR level at 89% and 56%, respectively, of the subway stations along their routes. During the process of responding to and recovering from waterlogging, the subway system performs better in the response-recovery stage than in the disaster prevention and diffusion stages. Therefore, it is necessary to strengthen disaster prevention and control work, specifically in the improvement of the natural environment and the construction and maintenance of infrastructure. Evaluating the SSWR is crucial for guiding resilience practices. Our research offers a widely applicable assessment framework and index

system for analyzing the SSWR under waterlogging conditions, yielding novel insights into the assessment of system resilience. These assessment results can help decision-makers develop more scientifically grounded strategies to enhance the subway system's resilience, mitigate the impact of waterlogging disasters, and further promote the sustainable development of subway systems.

Commencing at the station level, this study analyzes the SSWR and its driving factors, subsequently proposing an assessment framework and improvement measures for waterlogging resilience. Future research endeavors will extend beyond the station level to encompass the entire subway network, assessing its resilience across various failure scenarios and proposing strategies to bolster its overall resilience. Additionally, while this study has provided a robust framework for SSWR assessment, future research could benefit from advanced analysis methods such as Artificial Intelligence (AI). AI techniques could enable more sophisticated data analysis, pattern recognition, and predictive modeling, thereby offering more effective strategies for improving the resilience of subway systems against waterlogging disasters. This advancement could contribute significantly to the sustainable development and emergency preparedness of urban transit infrastructure.

CRediT authorship contribution statement

Fei Xu: Writing – original draft, Visualization, Methodology, Investigation, Data curation. **Delin Fang:** Writing – review & editing, Validation, Project administration, Funding acquisition, Conceptualization, Data curation, Investigation. **Bin Chen:** Project administration. **Hao Wang:** Validation, Conceptualization.

Declaration of competing interest

The authors declare that they have no known competing financial interests or personal relationships that could have appeared to influence the work reported in this paper.

Data availability

Data will be made available on request.

Acknowledgements

This work was supported by the National Natural Science Foundation of China (No. 72174029, 72091511), the Project Supported by State Key Laboratory of Earth Surface Processes and Resource Ecology (Project Number 2022-ZD-04), and the Fundamental Research Funds for the Central Universities.

Supplementary materials

Supplementary material associated with this article can be found, in the online version, at doi:10.1016/j.scs.2024.105710.

References

Alves, A., Gersonius, B., Kapelan, Z., Vojinovic, Z., & Sanchez, A. (2019). Assessing the Co-Benefits of green-blue-grey infrastructure for sustainable urban flood risk management. *Journal of Environmental Management, 239*, 244–254. https://doi.org/10.1016/j.jenvman.2019.03.036

Bera, M. K. (2023). Flood emergency management in a municipality in the Czech Republic: A study of local strategies and leadership. *Natural Hazards Research*. https://doi.org/10.1016/j.nhres.2023.06.004

Bruneau, M., Chang, S. E., Eguchi, R. T., Lee, G. C., O'Rourke, T. D., Reinhorn, A. M., Shinozuka, M., Tierney, K., Wallace, W. A., & von Winterfeldt, D. (2003). A Framework to Quantitatively Assess and Enhance the Seismic Resilience of Communities. *Earthquake Spectra, 19*, 733–752. https://doi.org/10.1193/1.1623497

Bruneau, M., & Reinhorn, A. (2007). Exploring the Concept of Seismic Resilience for Acute Care Facilities. *Earthquake Spectra, 23*, 41–62. https://doi.org/10.1193/1.2431396

Cao, F., Xu, X., Zhang, C., & Kong, W. (2023). Evaluation of urban flood resilience and its Space-Time Evolution: A case study of Zhejiang Province. *China. Ecological Indicators, 154*, Article 110643. https://doi.org/10.1016/j.ecolind.2023.110643

Ceola, S., Laio, F., & Montanari, A. (2014). Satellite night-time lights reveal increasing human exposure to floods worldwide. *Geophysical Research Letters, 41*. https://doi.org/10.1002/2014GL061859

Charnes, A., Cooper, W. W., & Rhodes, E. (1978). Measuring the efficiency of decision making units. *European Journal of Operational Research, 2*, 429–444. https://doi.org/10.1016/0377-2217(78)90138-8

Chen, P. (2021). Effects of the entropy weight on TOPSIS. *Expert Systems with Applications, 168*, Article 114186. https://doi.org/10.1016/j.eswa.2020.114186

Cimellaro, G. P., Reinhorn, A. M., & Bruneau, M. (2010). Framework for analytical quantification of disaster resilience. *Engineering Structures, 32*, 3639–3649. https://doi.org/10.1016/j.engstruct.2010.08.008

Coles, D., Yu, D., Wilby, R. L., Green, D., & Herring, Z. (2017). Beyond 'flood hotspots': Modelling emergency service accessibility during flooding in York. *UK. Journal of Hydrology, 546*, 419–436. https://doi.org/10.1016/j.jhydrol.2016.12.013

D'Ambrosio, R., & Longobardi, A. (2023). Adapting drainage networks to the urban development: An assessment of different integrated approach alternatives for a sustainable flood risk mitigation in Northern Italy. *Sustainable Cities and Society, 98*, Article 104856. https://doi.org/10.1016/j.scs.2023.104856

Damodaram, C., & Zechman, E. M. (2013). Simulation-Optimization Approach to Design Low Impact Development for Managing Peak Flow Alterations in Urbanizing Watersheds. *Journal of Water Resources Planning and Management, 139*, 290–298. https://doi.org/10.1061/(ASCE)WR.1943-5452.0000251

Deng, J. L. (1989). Introduction to Grey System Theory. *J. Grey Syst., 1*, 1–24.

Du, J., Qian, L., Rui, H., Zuo, T., Zheng, D., Xu, Y., & Xu, C.-Y. (2012). Assessing the effects of urbanization on annual runoff and flood events using an integrated hydrological modeling system for Qinhuai River basin. *China. Journal of Hydrology, 464–465*, 127–139. https://doi.org/10.1016/j.jhydrol.2012.06.057

Du, S., Shi, P., Van Rompaey, A., & Wen, J. (2015). Quantifying the impact of impervious surface location on flood peak discharge in urban areas. *Natural Hazards, 76*, 1457–1471. https://doi.org/10.1007/s11069-014-1463-2

Ekmekcioğlu, Ö., Koc, K., & Özger, M. (2022). Towards flood risk mapping based on multi-tiered decision making in a densely urbanized metropolitan city of Istanbul. *Sustainable Cities and Society, 80*, Article 103759. https://doi.org/10.1016/j.scs.2022.103759

Fang, C., Chu, Y., Fu, H., & Fang, Y. (2022). On the resilience assessment of complementary transportation networks under natural hazards. *Transportation Research Part D: Transport and Environment, 109*, Article 103331. https://doi.org/10.1016/j.trd.2022.103331

Feng, B., Zhang, Y., & Bourke, R. (2021). Urbanization impacts on flood risks based on urban growth data and coupled flood models. *Natural Hazards, 106*, 613–627. https://doi.org/10.1007/s11069-020-04480-0

Feng, T., & Zeng, X. (2024). Urban transportation system toughness assessment under New Crown epidemics. *PLOS ONE, 19*, 1–19. https://doi.org/10.1371/journal.pone.0300652

Forero-Ortiz, E., Martínez-Gomariz, E., Cañas Porcuna, M., Locatelli, L., & Russo, B. (2020). Flood Risk Assessment in an Underground Railway System under the Impact of Climate Change—A Case Study of the Barcelona Metro. *Sustainability, 12*. https://doi.org/10.3390/su12135291

Francis, R., & Bekera, B. (2014). A metric and frameworks for resilience analysis of engineered and infrastructure systems. *Reliability Engineering & System Safety, 121*, 90–103. https://doi.org/10.1016/j.ress.2013.07.004

Gao, W., Hu, X., & Wang, N. (2024). Resilience analysis in road traffic systems to rainfall events: Road environment perspective. *Transportation Research Part D: Transport and Environment, 126*, Article 104000. https://doi.org/10.1016/j.trd.2023.104000

Goldbeck, N., Angeloudis, P., & Ochieng, W. Y. (2019). Resilience assessment for interdependent urban infrastructure systems using dynamic network flow models. *Reliability Engineering & System Safety, 188*, 62–79. https://doi.org/10.1016/j.ress.2019.03.007

Han, Y., Liu, J., Li, J., Jiang, Z., Ma, B., Chu, C., & Geng, Z. (2023). Novel risk assessment model of food quality and safety considering physical-chemical and pollutant indexes based on coefficient of variance integrating entropy weight. *Science of The Total Environment, 877*, Article 162730. https://doi.org/10.1016/j.scitotenv.2023.162730

Hosseini, S., Barker, K., & Ramirez-Marquez, J. E. (2016). A review of definitions and measures of system resilience. *Reliability Engineering & System Safety, 145*, 47–61. https://doi.org/10.1016/j.ress.2015.08.006

Huang, H., Zhang, D., & Huang, Z. (2022). Resilience of city underground infrastructure under multi-hazards impact: From structural level to network level. *Resilient Cities and Structures, 1*, 76–86. https://doi.org/10.1016/j.rcns.2022.07.003

Hwang, C.L., Yoon, K., 1981. Multiple attribute decision making: Methods and applications.

Jiao, L., Zhu, Y., Huo, X., Wu, Y., & Zhang, Y. (2023). Resilience assessment of metro stations against rainstorm disaster based on cloud model: a case study in Chongqing, China. *Nat Hazards (Dordr), 116*, 2311–2337. https://doi.org/10.1007/s11069-022-05765-2

Jin, X. Y., Fang, D. L., Chen, B., & Wang, H. (2024). Multiobjective layout optimization for low impact development considering its ecosystem services. *Resources, Conservation and Recycling, 209*, 107794. https://doi.org/10.1016/j.resconrec.2024.107794

Jr, C. L. A., & Gibbons, C. J. (1996). Impervious Surface Coverage: The Emergence of a Key Environmental Indicator. *Journal of the American Planning Association, 62*, 243–258. https://doi.org/10.1080/01944369608975688

Kodag, S., Mani, S. K., Balamurugan, G., & Bera, S. (2022). Earthquake and flood resilience through spatial Planning in the complex urban system. *Progress in Disaster Science, 14*, Article 100219. https://doi.org/10.1016/j.pdisas.2022.100219

Kotzee, I., & Reyers, B. (2016). Piloting a social-ecological index for measuring flood resilience: A composite index approach. *Ecological Indicators, 60*, 45–53. https://doi.org/10.1016/j.ecolind.2015.06.018

Kuehler, E., Hathaway, J., & Tirpak, A. (2017). Quantifying the benefits of urban forest systems as a component of the green infrastructure stormwater treatment network. *Ecohydrology, 10*, e1813. https://doi.org/10.1002/eco.1813

Lin, S.-S., Zhou, A., & Shen, S.-L. (2023). Optimal construction method evaluation for underground infrastructure construction. *Automation in Construction, 152*, Article 104921. https://doi.org/10.1016/j.autcon.2023.104921

Lin, T., Liu, X., Song, J., Zhang, G., Jia, Y., Tu, Z., Zheng, Z., & Liu, C. (2018). Urban waterlogging risk assessment based on internet open data: A case study in China. *Habitat International, 71*, 88–96. https://doi.org/10.1016/j.habitatint.2017.11.013

Liu, J., Xiong, J., Chen, Y., Sun, H., Zhao, X., Tu, F., & Gu, Y. (2023). An integrated model chain for future flood risk prediction under land-use changes. *Journal of Environmental Management, 342*, Article 118125. https://doi.org/10.1016/j.jenvman.2023.118125

Liu, Z., Chen, H., Liu, E., & Hu, W. (2022). Exploring the resilience assessment framework of urban road network for sustainable cities. *Physica A: Statistical Mechanics and its Applications, 586*, Article 126465. https://doi.org/10.1016/j.physa.2021.126465

Longbin, K., & Hanping, Z. (2024). Regional resilience assessment based on city network risk propagation and cooperative recovery. *Cities, 147*, Article 104856. https://doi.org/10.1016/j.cities.2024.104856

Lu, X., Chan, F. K. S., Chen, W.-Q., Chan, H. K., & Gu, X. (2022). An overview of flood-induced transport disruptions on urban streets and roads in Chinese megacities: Lessons and future agendas. *Journal of Environmental Management, 321*, Article 115991. https://doi.org/10.1016/j.jenvman.2022.115991

Lyu, H.-M., Shen, S.-L., Yang, J., & Yin, Z.-Y. (2019). Inundation analysis of metro systems with the storm water management model incorporated into a geographical information system: a case study in Shanghai. *Hydrology and Earth System Sciences, 23*, 4293–4307. https://doi.org/10.5194/hess-23-4293-2019

Lyu, Hai-Min, Shen, S.-L., Zhou, A., & Yang, J. (2019a). Perspectives for flood risk assessment and management for mega-city metro system. *Tunnelling and Underground Space Technology, 84*, 31–44. https://doi.org/10.1016/j.tust.2018.10.019

Lyu, Hai-Min, Shen, S.-L., Zhou, A.-N., & Zhou, W.-H. (2019b). Flood risk assessment of metro systems in a subsiding environment using the interval FAHP-FCA approach. *Sustainable Cities and Society, 50*, Article 101682. https://doi.org/10.1016/j.scs.2019.101682

Lyu, H.-M., Sun, W.-J., Shen, S.-L., & Arulrajah, A. (2018). Flood risk assessment in metro systems of mega-cities using a GIS-based modeling approach. *Science of The Total Environment, 626*, 1012–1025. https://doi.org/10.1016/j.scitotenv.2018.01.138

Lyu, H.-M., Zhou, W.-H., Shen, S.-L., & Zhou, A.-N. (2020). Inundation risk assessment of metro system using AHP and TFN-AHP in Shenzhen. *Sustainable Cities and Society, 56*, Article 102103. https://doi.org/10.1016/j.scs.2020.102103

Ma, F., Ao, Y., Wang, X., He, H., Liu, Q., Yang, D., & Gou, H. (2023). Assessing and enhancing urban road network resilience under rainstorm waterlogging disasters. *Transportation Research Part D: Transport and Environment, 123*, Article 103928. https://doi.org/10.1016/j.trd.2023.103928

Mård, J., Baldassarre, G. D., & Mazzoleni, M. (2018). Nighttime light data reveal how flood protection shapes human proximity to rivers. *Science Advances, 4*, eaar5779. https://doi.org/10.1126/sciadv.aar5779

Martello, M. V., Whittle, A. J., Keenan, J. M., & Salvucci, F. P. (2021). Evaluation of climate change resilience for Boston's rail rapid transit network. *Transportation Research Part D: Transport and Environment, 97*, Article 102908. https://doi.org/10.1016/j.trd.2021.102908

National Bureau of Statistics of China. Beijing Statistical Yearbook 2022. Beijing: China Statistics Press. (In Chinese).

Nishant, Y., Samrat, C., & R, G. A. (2020). Resilience of Urban Transport Network-of-Networks under Intense Flood Hazards Exacerbated by Targeted Attacks. *Scientific reports, 10*, 10350.

Peng, Y., Zheng, R., Yuan, T., Cheng, L., & You, J. (2023). Evaluating perception of community resilience to typhoon disasters in China based on grey relational TOPSIS model. *International Journal of Disaster Risk Reduction, 84*, Article 103468. https://doi.org/10.1016/j.ijdrr.2022.103468

Qi, X., & Zhang, Z. (2022). Assessing the urban road waterlogging risk to propose relative mitigation measures. *Science of The Total Environment, 849*, Article 157691. https://doi.org/10.1016/j.scitotenv.2022.157691

Qiao, Y.-K., Peng, F.-L., Dong, Y.-H., & Lu, C.-F. (2024). Planning an adaptive reuse development of underutilized urban underground infrastructures: A case study of Qingdao. *China. Underground Space, 14*, 18–33. https://doi.org/10.1016/j.undsp.2023.05.005

Santos, P. P., Pereira, S., Zêzere, J. L., Tavares, A. O., Reis, E., Garcia, R. A. C., & Oliveira, S. C. (2020). A comprehensive approach to understanding flood risk drivers at the municipal level. *Journal of Environmental Management, 260*, Article 110127. https://doi.org/10.1016/j.jenvman.2020.110127

Shannon, C. E. (1948). A mathematical theory of communication. *The Bell System Technical Journal, 27*, 379–423. https://doi.org/10.1002/j.1538-7305.1948.tb01338.x

Shi, Q., Liu, M., Marinoni, A., & Liu, X. (2023). UGS-1m: fine-grained urban green space mapping of 31 major cities in China based on the deep learning framework. *Earth System Science Data, 15*, 555–577. https://doi.org/10.5194/essd-15-555-2023

Shi, Y., Yao, Q., Wen, J., Xi, J., Li, H., & Wang, Q. (2022). A spatial accessibility assessment of urban tourist attractions emergency response in Shanghai. *International Journal of Disaster Risk Reduction, 74*, Article 102919. https://doi.org/10.1016/j.ijdrr.2022.102919

Singh, A., Dawson, D., Trigg, M. A., Wright, N., Seymour, C., & Ferriday, L. (2023). Drainage representation in flood models: Application and analysis of capacity assessment framework. *Journal of Hydrology, 622*, Article 129718. https://doi.org/10.1016/j.jhydrol.2023.129718

Sohn, W., Brody, S. D., Kim, J.-H., & Li, M.-H. (2020). How effective are drainage systems in mitigating flood losses? *Cities, 107*, Article 102917. https://doi.org/10.1016/j.cities.2020.102917

Wang, G., Liu, L., Shi, P., Zhang, G., & Liu, J. (2021a). Flood Risk Assessment of Metro System Using Improved Trapezoidal Fuzzy AHP: A Case Study of Guangzhou. *Remote Sensing, 13*. https://doi.org/10.3390/rs13245154

Wang, G., Liu, Y., Hu, Z., Zhang, G., Liu, J., Lyu, Y., Gu, Y., Huang, X., Zhang, Q., & Liu, L. (2021b). Flood Risk Assessment of Subway Systems in Metropolitan Areas under Land Subsidence Scenario: A Case Study of Beijing. *Remote Sensing, 13*. https://doi.org/10.3390/rs13040637

Wang, Y., Xie, X., Liang, S., Zhu, B., Yao, Y., Meng, S., & Lu, C. (2020). Quantifying the response of potential flooding risk to urban growth in Beijing. *Science of The Total Environment, 705*, Article 135868. https://doi.org/10.1016/j.scitotenv.2019.135868

Wu, H.-L., Cheng, W.-C., Shen, S.-L., Lin, M.-Y., & Arulrajah, A. (2020). Variation of hydro-environment during past four decades with underground sponge city planning to control flash floods in Wuhan, China: An overview. *Underground Space, 5*, 184–198. https://doi.org/10.1016/j.undsp.2019.01.003

Xiao, H., Zhang, J., Xu, M., & Zhang, H. (2023). Study on spatial variability evaluation of hydrometeorological elements based on TOPSIS model. *Journal of Hydrology, 619*, Article 129359. https://doi.org/10.1016/j.jhydrol.2023.129359

Xiao, S., Zou, L., Xia, J., Dong, Y., Yang, Z., & Yao, T. (2023). Assessment of the urban waterlogging resilience and identification of its driving factors: A case study of Wuhan City. *China. Science of The Total Environment, 866*, Article 161321. https://doi.org/10.1016/j.scitotenv.2022.161321

Xie, T., Wang, M., Su, C., & Chen, W. (2018). Evaluation of the natural attenuation capacity of urban residential soils with ecosystem-service performance index (EPX) and entropy-weight methods. *Environmental Pollution, 238*, 222–229. https://doi.org/10.1016/j.envpol.2018.03.013

Yang, Junwen, Duan, C., Wang, H., & Chen, B. (2023). Spatial supply-demand balance of green space in the context of urban waterlogging hazards and population agglomeration. *Resources, Conservation and Recycling, 188*, Article 106662. https://doi.org/10.1016/j.resconrec.2022.106662

Yang, K., Hou, H., Li, Y., Chen, Y., Wang, L., Wang, P., & Hu, T. (2022). Future urban waterlogging simulation based on LULC forecast model: A case study in Haining City. *China. Sustainable Cities and Society, 87*, Article 104167. https://doi.org/10.1016/j.scs.2022.104167

Yang, T., Zhang, Q., Wan, X., Li, X., Wang, Y., & Wang, W. (2020). Comprehensive ecological risk assessment for semi-arid basin based on conceptual model of risk response and improved TOPSIS model-a case study of Wei River Basin. *China. Science of The Total Environment, 719*, Article 137502. https://doi.org/10.1016/j.scitotenv.2020.137502

Yang, Zhuyu, Barroca, B., Weppe, A., Bony-Dandrieux, A., Laffréchine, K., Daclin, N., November, V., Omrane, K., Kamissoko, D., Benaben, Frederick, Dolidon, H., Tixier, J., & Chapurlat, V. (2023). Indicator-based resilience assessment for critical infrastructures – A review. *Safety Science, 160*, Article 106049. https://doi.org/10.1016/j.ssci.2022.106049

Yang, Zhen, Dong, X., & Guo, L. (2023). Scenario inference model of urban metro system cascading failure under extreme rainfall conditions. *Reliability Engineering & System Safety, 229*, Article 108888. https://doi.org/10.1016/j.ress.2022.108888

Yolina, H., Rojali, & Irwansyah, E (2023). Development of flood-prone area classification program using linear classifier method based on geomorphic flood index and land cover. *Procedia Computer Science, 216*, 396–405. https://doi.org/10.1016/j.procs.2022.12.151

Yu, D., Yin, J., Wilby, R. L., Lane, S. N., Aerts, J. C. J. H., Lin, N., Liu, M., Yuan, H., Chen, J., Prudhomme, C., Guan, M., Baruch, A., Johnson, C. W. D., Tang, X., Yu, L., & Xu, S. (2020). Disruption of emergency response to vulnerable populations during floods. *Nature Sustainability, 3*, 728–736. https://doi.org/10.1038/s41893-020-0516-7

Yu, S., Kong, X., Wang, Q., Yang, Z., & Peng, J. (2023a). A new approach of Robustness-Resistance-Recovery (3Rs) to assessing flood resilience: A case study in Dongting Lake Basin. *Landscape and Urban Planning, 230*, Article 104605. https://doi.org/10.1016/j.landurbplan.2022.104605

Yu, S., Yuan, M., Wang, Q., Corcoran, J., Xu, Z., & Peng, J. (2023b). Dealing with urban floods within a resilience framework regarding disaster stages. *Habitat International, 136*, Article 102783. https://doi.org/10.1016/j.habitatint.2023.102783

Zadeh, L. A. (1968). Fuzzy algorithms. *Information and Control, 12*, 94–102. https://doi.org/10.1016/S0019-9958(68)90211-8

Zhang, L., Chen, T., Liu, Z., Yu, B., & Wang, Y. (2024). Analysis of multi-modal public transportation system performance under metro disruptions: A dynamic resilience assessment framework. *Transportation Research Part A: Policy and Practice, 183*, Article 104077. https://doi.org/10.1016/j.tra.2024.104077

Zhang, M., Xu, M., Wang, Z., & Lai, C. (2021). Assessment of the vulnerability of road networks to urban waterlogging based on a coupled hydrodynamic model. *Journal of Hydrology, 603*, Article 127105. https://doi.org/10.1016/j.jhydrol.2021.127105

Zhang, Yongling, Li, X., Kong, N., Zhou, M., & Zhou, X. (2022). Spatial Accessibility Assessment of Emergency Response of Urban Public Services in the Context of Pluvial Flooding Scenarios: The Case of Jiaozuo Urban Area. *China. Sustainability, 14*. https://doi.org/10.3390/su142416332

Zhang, Yao, Zhang, Yongjian, Zhang, H., & Zhang, Yuxin (2022). Evaluation on new first-tier smart cities in China based on entropy method and TOPSIS. *Ecological Indicators, 145*, Article 109616. https://doi.org/10.1016/j.ecolind.2022.109616

Zhao, B., Tang, Y., Wang, C., Zhang, S., & Soga, K. (2022). Evaluating the flooding level impacts on urban metro networks and travel demand: behavioral analyses, agent-based simulation, and large-scale case study. *Resilient Cities and Structures, 1*, 12–23. https://doi.org/10.1016/j.rcns.2022.10.004

Zhao, J., Ke, E., Wang, B., & Zhao, Y. (2024). An optimization model for the impervious surface spatial layout considering differences in hydrological unit conditions for urban waterlogging prevention in urban renewal. *Ecological Indicators, 158*, Article 111546. https://doi.org/10.1016/j.ecolind.2024.111546

Zhao, J., Yang, F., Guo, Y., & Ren, X. (2022). A CAST-Based Analysis of the Metro Accident That Was Triggered by the Zhengzhou Heavy Rainstorm Disaster. *International Journal of Environmental Research and Public Health, 19*. https://doi.org/10.3390/ijerph191710696

ZHAO, S., YANG, X., DAI, T., & ZHANG, C. (2020). Within-Day Variation of the Complexity of Bus Passenger Flow Network based on Smart Card Data. *Journal of Geo-information Science, 22*, 1254.

Zhao, Y., & Zhou, Y. (2023). Identification of the critical hospitals in the urban post-disaster healthcare system based on the network modeling and multi-criteria decision-making. *International Journal of Disaster Risk Reduction, 93*, Article 103795. https://doi.org/10.1016/j.ijdrr.2023.103795

Zhe, W., Xigang, X., & Feng, Y. (2021). An abnormal phenomenon in entropy weight method in the dynamic evaluation of water quality index. *Ecological Indicators, 131*, Article 108137. https://doi.org/10.1016/j.ecolind.2021.108137

Zheng, J., & Huang, G. (2023). Towards flood risk reduction: Commonalities and differences between urban flood resilience and risk based on a case study in the Pearl River Delta. *International Journal of Disaster Risk Reduction, 86*, Article 103568. https://doi.org/10.1016/j.ijdrr.2023.103568

Zheng, Q., Shen, S.-L., Zhou, A., & Lyu, H.-M. (2022). Inundation risk assessment based on G-DEMATEL-AHP and its application to Zhengzhou flooding disaster. *Sustainable Cities and Society, 86*, Article 104138. https://doi.org/10.1016/j.scs.2022.104138

Zhou, Y., Li, Zihao, Meng, Y., Li, Zhongwen, & Zhong, M. (2021). Analyzing spatio-temporal impacts of extreme rainfall events on metro ridership characteristics. *Physica A: Statistical Mechanics and its Applications, 577*, Article 126053. https://doi.org/10.1016/j.physa.2021.126053

Zhu, S., Li, D., Feng, H., & Zhang, N. (2023). The influencing factors and mechanisms for urban flood resilience in China: From the perspective of social-economic-natural complex ecosystem. *Ecological Indicators, 147*, Article 109959. https://doi.org/10.1016/j.ecolind.2023.109959

Ziari, K., Ebrahimipour, M., & Ardalan, D. (2023). Physical resilience of riverside cities against floods. *Environmental Science & Policy, 148*, Article 103548. https://doi.org/10.1016/j.envsci.2023.07.008